Lawrence Berkeley National Laboratory
Recent Work

Title
Zinc Air Battery Development for Electric Vehicles

Permalink
https://escholarship.org/uc/item/1kf7g8fq

Authors
Putt, R.A.
Merry, G.W.

Publication Date
1991-07-01
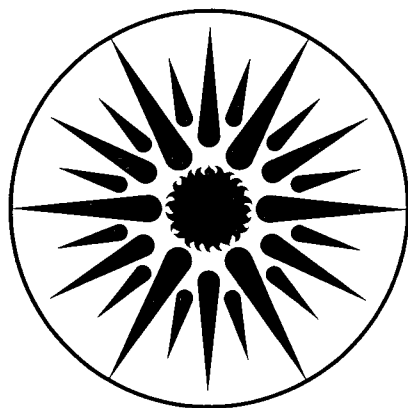
Lawrence Berkeley Laboratory

UNIVERSITY OF CALIFORNIA

APPLIED SCIENCE
DIVISION

Zinc Air Battery Development for Electric Vehicles

R.A. Putt and G.W. Merry

July 1991

**APPLIED SCIENCE
DIVISION**

DISCLAIMER

ZINC AIR BATTERY DEVELOPMENT

FOR ELECTRIC VEHICLES

Final Report

July 1991

by

Ronald A. Putt

Glenn W. Merry

MATSI, Inc.
430 Tenth Street, NW
Suite S-007
Atlanta, Georgia 30318-5768

for

Technology Base Research Project
Applied Science Division
Lawrence Berkeley Laboratory
Berkeley, California 94720

Table of Contents

EXECUTIVE SUMMARY

This report summarizes the results of research conducted during the sixteen month continuation of a program to develop rechargeable zinc-air batteries for electric vehicles.

The zinc-air technology under development incorporates a metal foam substrate for the zinc electrode, with flow of electrolyte through the foam during battery operation. In this "soluble" zinc electrode the zincate discharge product dissolves completely in the electrolyte stream. Cycle testing at Lawrence Berkeley Laboratory, where the electrode was invented, and at MATSI showed that this approach avoids the zinc electrode shape change phenomenon. Further, electrolyte flow has been shown to be necessary to achieve significant cycle life (>25 cycles) in this open system. Without it, water loss through the oxygen electrode results in high-resistance failure of the cell.

The Phase I program, which focussed entirely on the zinc electrode, elucidated the conditions necessary to increase electrode capacity from 75 to as much as 300 mAh/cm^2. In addition, it confirmed the effectiveness of CELGARD® 3401 (Celanese Corporation), in three layers, as a separator, and it identified a dense zinc preplate which protected the copper foam from corrosive attack in the cell. By the end of the Phase I program over 500 cycles had accrued on one of the zinc-zinc half cells undergoing continuous cycle testing. The Phase II program continued the half cell cycle testing and separator development, further refined the foam preplate process, and launched into performance and cycle life testing of zinc-air cells.

In the half cell testing we learned that pulse or steady charging of the zinc electrode at high current densities (50-100 ma/cm^2 per side) quickly results in dendrite penetration of the separator and internal shorting. Zinc, lead, and tin are acceptable preplate metals, while mercury produces severe electrode densification and shorting within a few cycles. Ethylene-propylene-diene monomer (EPDM) performs well as a gasket material in the system, while VITON® (DuPont Corporation) swells, embrittles, and cracks. High electrolyte concentration (45% KOH) produces soft, mossy zinc morphology in this soluble electrode, whereas low (<25%) concentrations produce hard, crystalline deposits. By the end of the program both zinc-zinc cycle test cells had achieved over 700 cycles on their zinc electrodes.

Results of the separator development task showed that the best electrode for this cell comprises two or more (preferably three) layers of CELGARD 3401 compressed sufficiently between electrodes to ensure firm facial contact of the layers, absent gaps or air pockets. Attempts to improve separator performance by adding interlayers of various absorbent materials were uniformly unsuccessful.

1

Further work on the copper foam preplating process yielded additional acceptable preplates, namely lead and tin-lead, to zinc. However, in all testing conducted there was no clear superiority of either preplate over dense zinc. Each successfully prevents corrosion of the copper foam and excessive hydrogen generation, and each is eventually dissolved during extended periods of cell reversal when the substrate is positive to the oxygen electrode potential. At this juncture dense zinc remains the preferred preplate, since it is a straightforward process and it does not employ acutely toxic heavy metals, as classified by the EPA.

Testing of zinc-air cells began with a three-electrode cell, in which there was an oxygen-evolving electrode for charge and an oxygen cathode for discharge, the two electrically isolated from one another. While this design worked very well for laboratory testing, it suffers from lower energy density, because of the need for a second flow loop to circulate through the oxygen anode, and complexity associated with electrically switching between the oxygen anode and cathode for charge and discharge, respectively. The three-electrode cell was displaced once efficient rechargeable, or bifunctional, oxygen electrodes became available. With these, oxygen formed during charge permeates the porous electrode structure and escapes to the air stream on the back side of the electrode, allowing the oxygen electrode to be placed firmly against the separator.

The oxygen electrodes tested during the program showed good performance and stability. They employed graphitized catalyst supports, which Lawrence Berkeley Laboratory has shown to be stable under oxygen evolution conditions, and spinel and porphyrin catalysts for the charge and discharge reactions, respectively. Zinc-air cells tested exhibited stable performance cycle to cycle in preliminary cycle testing, met the SFUDS duty cycle requirement, and demonstrated an electrolyte capacity of over 350 g/ℓ of zinc solubility, as compared with an original goal of 300 g/ℓ.

Our overall assessment of this soluble zinc electrode zinc-air system is that it avoids zinc electrode densification and dryout failure, as it was designed to do. The specific energy of the system is projected to be approximately 100 Wh/kg, which is competitive with any of the mid-term advanced batteries being developed for electric vehicle propulsion.

MATSI has further developed the technology by converting the zinc electrode to an insoluble form, while retaining the metal foam substrate structure and electrolyte flow. This has permitted reduction of electrolyte volume by 40%. Densification is minimized by employing low electrolyte concentration (3 M KOH), in combination with supporting electrolyte, which has been shown effective in nickel-zinc battery development efforts at Lawrence Berkeley Laboratory. Moreover, the flowing electrolyte/inert foam substrate combination permits periodic maintenance cycles in which the zinc deposit may be completely stripped and replaced, thereby renewing the zinc electrodes *in situ*. This insoluble form of the zinc electrode produces a projected battery specific energy of over

2

180 Wh/kg, which is the highest specific energy of all rechargeable aqueous battery systems and which is fully competitive with all intermediate and high temperature lithium systems.

INTRODUCTION

This report summarizes the results of research conducted during the sixteen month continuation of a program to develop zinc-air batteries for electric vehicles. The results of the first phase of this program are contained in Reference 1. This section will provide a brief review of the technology studied.

The electrode reactions for the zinc-air couple on discharge are as follows:

			E^o (25° C)
Negative:	$Zn + 2OH^-$	$\rightarrow Zn(OH)_2 + 2e$	-1.245 V
Positive:	$\frac{1}{2}O_2 + H_2O + 2e \rightarrow 2OH^-$		+0.401
Overall:	$Zn + \frac{1}{2}O_2 + H_2O \rightarrow Zn(OH)_2$		1.646 V

The high specific energy of zinc-air cells make them an attractive candidate for EV missions, but development has been frustrated to date by the shape change phenomenon (densification) exhibited by the zinc electrode. Furthermore, the capacity density (typically 30 mAh/cm^2) of the zinc electrode is limited to achieve a reasonable cycle life.

Lawrence Berkeley Laboratory has developed a novel design for the zinc electrode to overcome these limitations. In this approach an open-cell metal foam substrate is employed for the zinc electrode, through which the electrolyte is circulated during battery operation (Figure 1). Zinc, which is dissolved in the electrolyte as zincate ions, deposits electrochemically onto the filaments of the foam during charge and redissolves into the electrolyte during discharge. The flowing electrolyte supplies and removes the zincate specie uniformly during charge and discharge, respectively, thus avoiding densification. Electrolyte flow is also required in the zinc-air system to prevent localized dryout caused by water evaporation into the air stream.
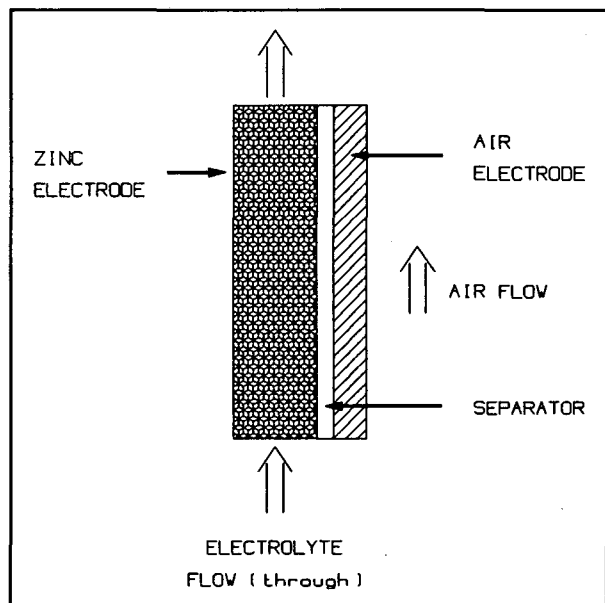

Figure 1: Rechargeable Cell Design Concept

In Phase I of the present program MATSI transitioned the technology from LBL into an industrial development setting, with an emphasis on verifying the cycle capability of the zinc electrode. Phase I was very successful in this regard; cycle testing on zinc-zinc half-cells proceeded beyond eight hundred cycles with steady performance and no incidence of densification. Further, the achievable capacity density was increased to 240 mAh/cm^2, an eight-fold increase as compared with the insoluble zinc electrode in a stationary electrolyte.

Additional findings of the Phase I effort were as follows:

• Zinc Deposit Morphology: The zinc deposit morphology, for charge current densities in the range 1-10 mA/cm^2, is soft and mossy, with a high specific surface area which is very active electrochemically. It is concentrated at the front face of the metal foam substrate, with a penetration depth of less than 2 mm at loadings of up to 150 mAh/cm^2 per side. The pore structure becomes completely filled by mossy zinc at loadings greater than 100 mAh/cm^2 per side.

• Substrate Preparation: The copper foam substrate must be protected from corrosion during cell cycling, otherwise excessive hydrogen gassing will occur and a corrosion layer develops on the copper, which becomes electrochemically inactive. Initial success in protecting the substrate was achieved with dense zinc.

• Separator Selection: A separator with excellent dendrite resistance properties is required. After evaluation of several alternatives, Celgard® 3401 was found to be the only material resistant to dendrite penetration.

In Phase II, which is reported on herein, the half-cell cycle testing program was continued, and new tasks were added to focus effort in the areas of separator and negative electrode preplate development, to begin cycle testing of zinc-air cells, and to study the effects of scale-up on zinc deposit morphology.

PHASE II PROGRAM

The Phase II program comprised five tasks, as follows:

• Task 1:   Half-Cell Studies
• Task 2:   Separator Development
• Task 3:   Negative Electrode Preplate
• Task 4:   Zinc-Air Cell Testing
• Task 5:   Scale-up Effects

Task 5 was discontinued early in the program based upon initial results which indicated that zinc electrode performance was insensitive to increased length, at least up to 15 cm. Results for the remaining four tasks are presented below.

5

HALF-CELL STUDIES

The purpose of the half-cell studies was to demonstrate the cycle capability of the zinc electrode and to identify proper materials, electrolyte formulations, and operating conditions for good efficiency and trouble-free cycling.

The zinc-zinc cell design (Figure 2), developed during Phase I, was used for these studies as well, and the cycle testing which began in Phase I was continued throughout Phase II for the two cycle test cells. The results of these studies are presented below.
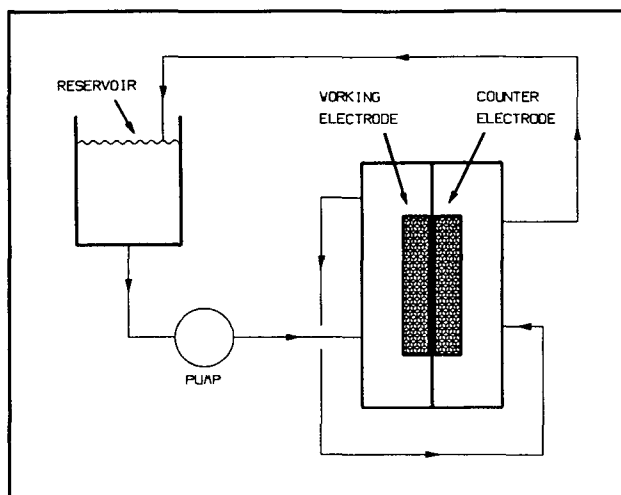

Figure 2: Zinc-Zinc Cell Test System

- Pulse charging at a pulse current density of 50-100 mA/cm^2 at a duty cycle of 10% and a frequency of 15 Hz is very detrimental to this zinc electrode. It results in a hard, crystalline morphology with dendrite growth that penetrates the Celgard separator. This morphology is typical of that obtained at high (>20 mA/cm^2) current densities, pulsed or steady. In contrast, limiting the maximum charge current density to 15 mA/cm^2 or less is conducive to the formation of a soft, mossy morphology which is desired.

- Metals in contact with the zinc electrode in the electrolyte must have a high overpotential for hydrogen evolution to ensure good current efficiency. These include lead, tin, tin-lead solder, silver, and zinc. There was an incidence of gradual loss of zinc plating on the steel screws used for current feedthroughs such that the steel became exposed. This led to high corrosion rates of the zinc active material and low current efficiencies. These screws were replaced with solder-coated brass screws, which eliminated the source of high corrosion.

  Mercury, which also has a high overpotential for hydrogen evolution, is to be avoided entirely in this system. It is very conducive to the formation of hard and dense zinc deposits which are not active electrochemically and which have a propensity for dendrite shorting.

- Ethylene-propylene-diene monomer (EPDM) is a stable and effective elastomer for gaskets and O-ring seals, whereas Viton, a fluoroelastomer, swells and cracks in concentrated KOH.

6

• High electrolyte concentrations (45%) are conducive to the formation of soft, mossy zinc morphology desired. We found that lower concentrations of the electrolyte (<25%) result in a dense, nodular morphology which is much less active electrochemically than the mossy morphology and which is conducive to dendrite penetration of the separator.

Test logs of the two zinc-zinc half cells are contained in Appendices A and B. At the end of the test program both cells continued to cycle. As of June 30, 1991, Cell #1 had 728, 592, and 342 cycles on the working electrode, counter electrode, and separator, respectively, and Cell #2 had 710, 602, and 26 cycles on its respective components.

SEPARATOR DEVELOPMENT

The separator must present an effective barrier to penetration by zinc dendrites, it must be stable with respect to the rechargeable oxygen electrode, and it must have a low resistance to ionic current. The half-cell studies of Phase I showed Celgard 3401 to be an effective dendrite barrier when the current density and negative electrode loading were kept within proper limits. The Phase II program included a separator study to evaluate Celgard 3401 against the other two criteria, *i.e.* stability to the oxygen electrode and low ionic resistance. The key findings of this study are as follows:

● One layer of Celgard 3401 is not sufficient as a dendrite barrier. The material apparently has minor imperfections distributed across its surface which allow penetration by zinc dendrites. Dendrite shorting was experienced in less than twenty cycles when only one layer was used. Two or more layers, on the other hand, are effective, because the likelihood of imperfections lining up layer-to-layer is very low. Dendrite penetration of two or more layers is only experienced if the current density or loading limit is exceeded or if the electrolyte composition is not conducive to the formation of a soft, mossy zinc morphology which is desired.

● Celgard is stable to the rechargeable oxygen electrode. In all testing performed on zinc-air cells there were no indications of Celgard degradation by the oxygen electrode during charge. The material remained structurally and electrochemically invariant.

● The use of two or more layers of Celgard requires that sufficient compression is achieved between layers to assure good facial contact. Otherwise, gaps or air pockets between layers result, which form regions of high ionic resistance that block current passage (Figure 3). Several methods were evaluated to ensure good contact between layers, including the use of interseparators and a bonding agent, with poor success.
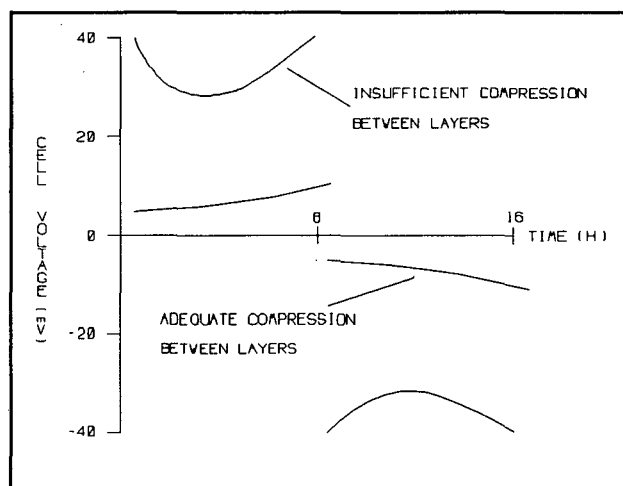

Figure 3: Charge-Discharge Curves for Zinc-Zinc Half Cells

Interseparators of an absorbent, non-woven material, specifically radiation-treated polypropylene (RAI PHDC-80),

polyvinyl alcohol (Chicopee 7601), and polyamide (Pellon 2527), were added, in separate experiments, between layers of Celgard 3401 to provide good conduction between layers. These interseparators were generally effective in preventing high resistance gaps, but they served as a substrate for zinc dendrite growth between layers. The zinc would penetrate through a flaw in the first layer of Celgard 3401, then grow laterally throughout the interseparator layer, until it found a flaw in the next layer of Celgard, which it would then penetrate. In this way, the interseparators would eventually lead to dendrite shorting between electrodes, making their use unacceptable.

Polyvinyl alcohol was evaluated as a bond between layers. The layers of Celgard were saturated with a 3% solution of PVA in water, then pressed together and dried. The resulting laminate worked satisfactorily for a few cycles, but gradually the PVA bond would break down and allow the Celgard layers to separate.

Finally, cell dimensions were adjusted to provide an interference fit between electrodes, thereby pressing the Celgard layers firmly together, as is practiced in nickel-zinc and silver-zinc battery technology. This proved to be an effective and reliable means of ensuring good facial contact between separator layers.

NEGATIVE ELECTRODE PREPLATE

Bare copper foam is not suitable as the negative electrode substrate for two reasons. First, copper has a lower overpotential for hydrogen evolution than zinc, such that electrodepositing zinc under normal charging conditions is precluded by the cathodic decomposition of water to hydrogen gas; the current efficiency for the zinc electrode is essentially zero. Second, if special steps are taken to allow the deposition of zinc, the copper substrate develops, within a few cycles, a dull brown corrosion layer which is electrochemically inactive, resulting in both poor voltage and current behavior.

In Phase I a preplating process was developed to provide a dense zinc coating of the copper foam. This preplate solved the problems with the bare copper substrate mentioned above, but it did not tolerate extended periods at the oxygen electrode potential after complete discharge of the negative electrode. It would slowly dissolve anodically at the oxygen electrode potential, which eventually would expose the copper substrate to anodic dissolution as well, thereby resulting in electrode failure.

In Phase II several other candidate preplates were evaluated for efficacy. These included lead, tin, cadmium, mercury, and tin-lead solder. The lead, tin, and cadmium, electrochemically plated onto the copper foam, were effective in preventing hydrogen gassing and substrate oxidation under normal conditions, but were no more resistant than zinc to anodic dissolution at the oxygen electrode potential. The mercury was applied by immersing the foam sample into liquid mercury underneath a fluxing solution of dilute nitric acid. The presence of mercury in the system, however, proved extremely deleterious to the morphology of the zinc electrodeposit. Instead of the soft, mossy structure, a very hard, crystalline, and dense structure was formed which was much less active electrochemically and which readily penetrated the Celgard separator. Because of this, mercury was removed from the list of candidate electrode preplates.

The tin-lead solder, applied in its molten state to the foam, demonstrated a reasonable degree of resistance to anodic dissolution at the oxygen electrode potential, and is therefore a candidate for further evaluation in an engineering development program. It, however, proved difficult to apply in a thin layer, adding excessive weight and volume to the substrate. Solder-application technology would have to be refined to provide a uniformly thin and contiguous coating of the copper foam filaments. Preliminary evaluation of a combination dense zinc – dense lead preplate, similar to that obtained with solder plate baths, was encouraging; it works at least as well as dense zinc alone, and its tolerance to brief overdischarge should be even better.

The dense zinc preplate was employed and further developed throughout Phase II since no better preplate was found. One major advantage to its use is that it does not introduce a foreign metal into the system, particularly since all the other candidate metals,

except tin, belong to the EPA's group of acutely toxic heavy metals. Under normal cell operating conditions, including deep discharge, the zinc preplate has demonstrated durability and efficacy in protecting the copper substrate. All of the zinc-zinc half-cells and the zinc-air cells tested in the program employed negative electrodes with a zinc preplate, and the only failures experienced were when the zinc electrodes were forced anodically beyond their capacities of electroactive zinc.

ZINC-AIR CELL TESTING

Cycle testing of the metal foam negative electrode in zinc-zinc half-cells has been very productive in identifying the proper design, materials selection, and operating parameters to ensure good electrode efficiency and cycle life. Once a baseline of performance was established on the half-cells, the next step was to test the negative electrode opposite the oxygen electrode in zinc-air cells.

Since there were no suitably efficient rechargeable oxygen electrodes available at the beginning of the Phase II effort, a three-electrode cell was developed (Figure 4) to allow zinc-air cycle testing to proceed. This cell had two oxygen electrodes, one for charge and one for discharge, which were electrically isolated from one another by a layer of separator material.

Figure 4: Three Electrode Cell Design Concept

The oxygen anode evolved oxygen during charge, which was carried away by a second electrolyte circulation system to an external reservoir where the oxygen was released to the atmosphere. The oxygen cathode reduced oxygen from the atmosphere during discharge. An electrical relay was employed to connect the zinc electrode and the oxygen anode to a constant-current power supply during charge, and the zinc electrode and the oxygen cathode to a load resistor during discharge.

Initially the oxygen anode comprised three layers of 0.3 mm thick expanded nickel foil, which performed satisfactorily. Later on, nickel foam (Retec, Eltech Research Corporation) was substituted when it became available, and it worked equally well and was easier to handle as one piece. The oxygen cathode was a PTFE-bonded carbon with a CoTMPP catalyst (AE-20, Electromedia Corporation). These electrodes required electrical isolation one from another within the cell, otherwise the anodic potential of the oxygen anode during charge would oxidize the carbon substrate of the oxygen cathode.

One layer of Celgard 5401 (a laminate of Celgard 3401 with a non-woven polypropylene web), placed between the two oxygen electrodes, performed well in the isolation function. The polarization behavior of the three-electrode cell during discharge is shown in Figure 5, in contrast to the polarization curve for a zinc-zinc half cell.
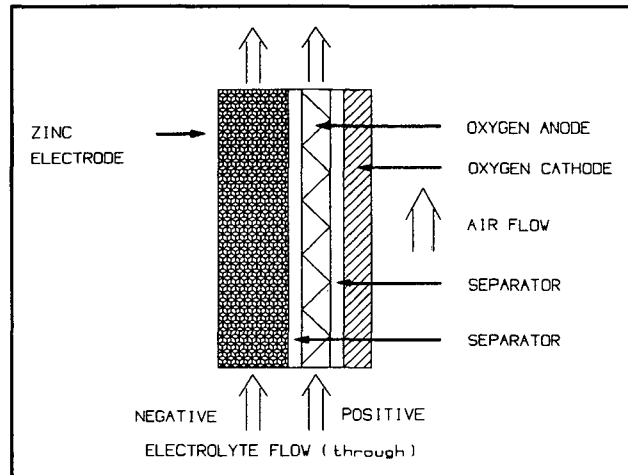
An efficient rechargeable oxygen electrode became available midway through the Phase II program. Designated BF-6 by the manufacturer (Electromedia Corporation) this electrode was similar in construction to the AE-20 air cathode, in that it was a PTFE-bonded carbon structure with a cobalt catalyst, but a recharge catalyst was added and the carbon substrate was graphitized to resist oxidation during the charge half-cycle. A two electrode zinc-air cell was assembled with a BF-6 oxygen electrode. In this cell the oxygen electrode was pressed against the zinc electrode, separated by three layers of Celgard 3401 and one layer of Celgard 5401. The oxygen formed during charge passed to the atmosphere through the pores of the oxygen electrode, and oxygen returned through these pores from the atmosphere to be consumed during discharge, thus obviating the second electrolyte circulation system which was required for the three-electrode cell.
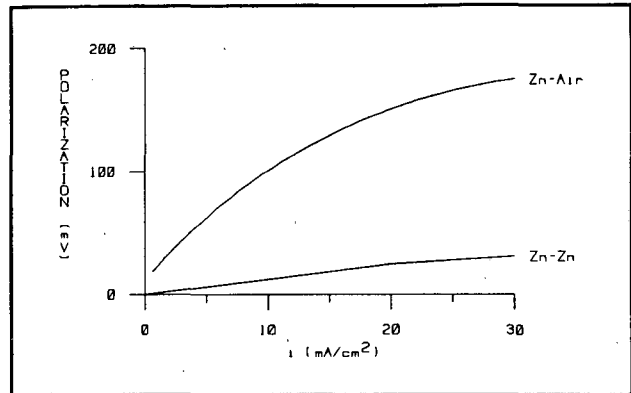
Figure 5: Polarization Behavior on Discharge

Testing of the three-electrode cell was performed during the first half of Phase II until the two-electrode cell was debugged and made fully operational. Both cells were tested with a dilute electrolyte (22% KOH) to minimize the carbonation reaction in the pores of the oxygen electrodes. Electrode failure (swelling and weeping) because of carbonation occurred within 7 days when 45% KOH was used, but the lower electrolyte concentration allowed months of testing before carbonation-related failure of this oxygen electrode.

Once the negative impact of the lower KOH concentration on zinc deposit morphology was discovered (i.e. dense, nodular growth, discussed under HALF-CELL STUDIES), the electrolyte concentration was increased to 45%. A closed-loop air recirculation system was developed to prevent exposure of the oxygen electrode to carbon dioxide (Figure 6). This system employed an air reservoir, consisting of a polypropylene bag, and a peristaltic pump to circulate air to the oxygen electrode. What little carbon dioxide which was contained in this volume was gradually dissolved by the electrolyte, and thereafter the air was essentially free of carbon dioxide. The implementation of the air recirculation system eliminated the carbonation failure mode for the oxygen electrode, and continuous testing was resumed.
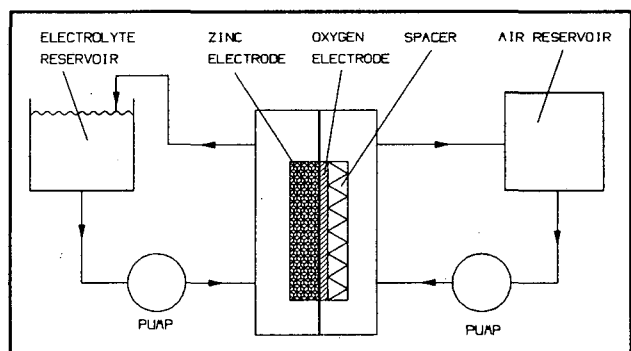
Figure 6: Zinc-Air Cell System

Edge effect dendrite shorting in the two-electrode cell was another short-term failure mode which required attention. This was caused by the imbalance between the charge and discharge current densities at the edges of the electrodes; the charge current density was much higher there than was the discharge current density.
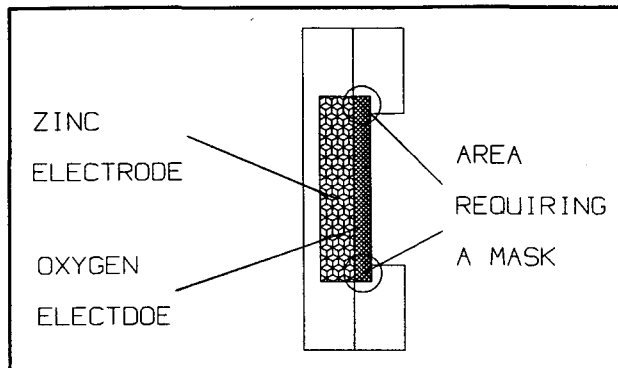

Figure 7: Edge Effect Scenario

The oxygen electrode was made to the same length and width dimensions as the zinc electrode, but it was bonded into a border recess (Figure 7) in the oxygen electrode frame which was 0.3 cm wide. The front side of the electrode, where the charge reaction occurs, was thus fully exposed to the zinc electrode, but the back side, which provided oxygen access for the discharge reaction, was smaller by the width of the border along each edge. Therefore, the zinc electrode was charged each cycle across its entire frontal surface, but a 0.3 cm border along all edges was discharged at only a fraction of the average discharge current density. This led to a buildup of zinc along the edges which eventually penetrated the separator and caused shorting there.

The solution to this problem was straightforward. An aperture of electrolyte-impermeable film (e.g. polypropylene), which was placed between the electrodes to mask the border during charge as well as discharge, proved effective; edge effect dendrites ceased to be a problem with this aperture in place.

Elimination of the carbonation and edge effect dendrite problems permitted continuous cycle testing to proceed. A typical charge-discharge curve is shown in Figure 8, and a voltage-current curve is shown in Figure 9. The voltage profiles are flat during charge and discharge, and the voltage-current behavior is fairly linear to a current density of at least 40 mA/cm^2, the design limit.
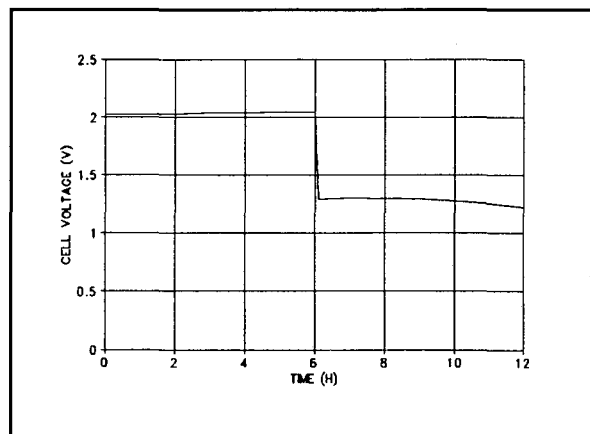

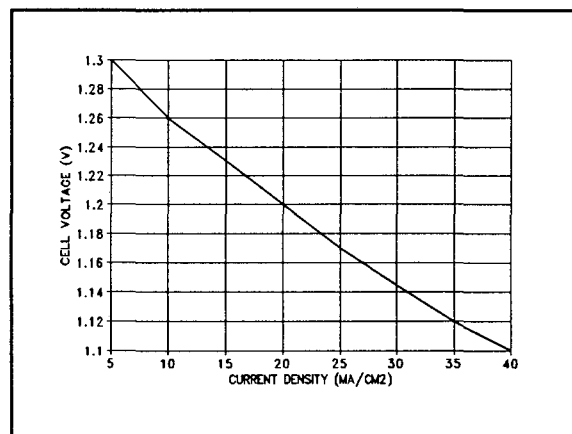Figure 8: Cell Charge-Discharge Curve

Figure 9: Cell Voltage-Current Curve

The average charge and discharge voltages are shown in Figure 10 for the 50 cycles of this test.

Electrolyte Capacity Testing

The zinc-air cell testing program was extended to enhance the solubility of zincate ions in the electrolyte. The zincate solubility must be at least 300 g/ℓ (as zinc) to achieve the specific energy and energy density goals of the EV program (Figures 11 and 12). However, the solubility of zincate ions in 45% KOH is less than 100 g/ℓ (as zinc), and zincate supersaturation falls short of the 300 g/ℓ goal. Therefore, increasing the solubility is required.
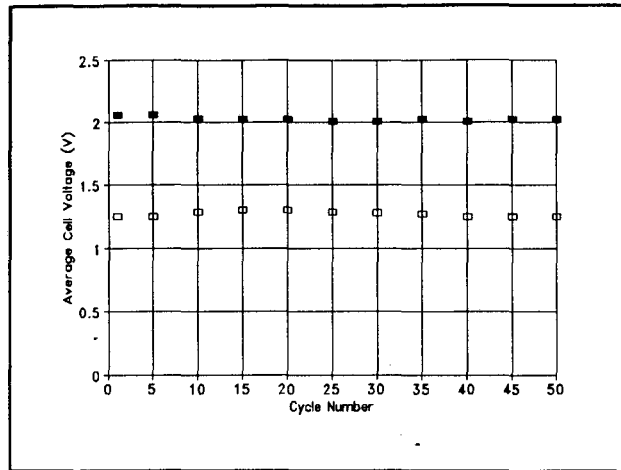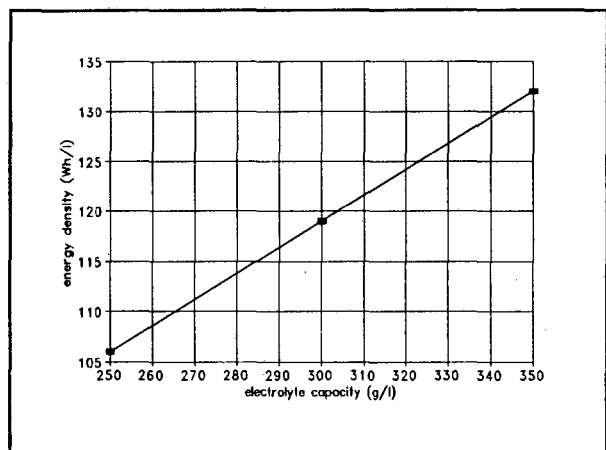
Figure 10:   Cell Cycle Test Data

Figure 11:   Energy Density Sensitivity
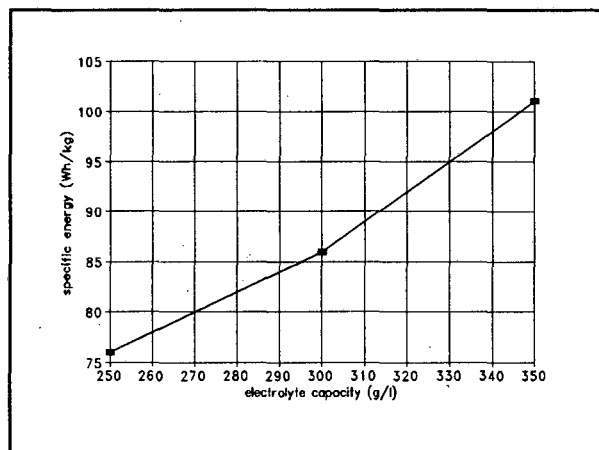
Figure 12:   Specific Energy Sensitivity

There were two extenders, silicate and lithium hydroxide, reported in the literature (References 2 and 3) which were considered to be worthy of evaluation. For their evaluation, a special cell was built (Figure 13) which would produce enough zincate during discharge to reach the desired concentration of zinc in the electrolyte. The cell employed a zinc anode consisting of zinc shot, through which the electrolyte was circulated during discharge. The cathode was AE-20 (Electromedia Corporation), and the separator was one layer of Celgard 5401. The volume of

Figure 13:   Zinc Shot Cell

electrolyte, 25 ml, was the minimum required to fill the cell and the circulation system, with a small excess in the reservoir.

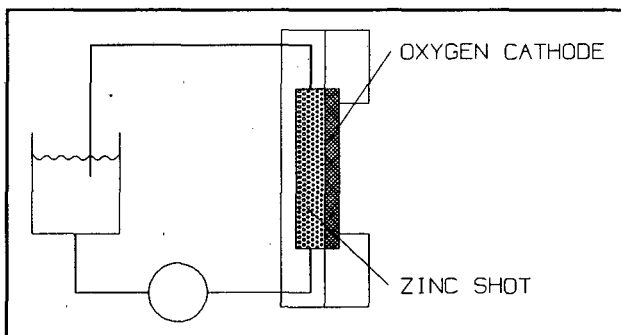Three runs were conducted, one with 45% KOH only, one with 45% KOH plus 25 g/ℓ of silicate (added as sodium metasilicate), and one with 45% KOH plus 20 g/ℓ lithium hydroxide. For each run the cell was discharged through a fixed resistor until the zinc was depleted to the point that it could no longer sustain the discharge voltage. In the run with KOH only, precipitation was evident just before the 300 g/ℓ mark. In the run with silicate, there was no precipitation throughout the run, to a concentration of over 380 g/ℓ. However, on stand there was an accumulation of white precipitate in the bottom of the reservoir. In the run with lithium hydroxide, there was no precipitation throughout the run, also to a concentration of over 380 g/ℓ, and there was no precipitation on stand. Based on these observations, the lithium hydroxide additive appears superior to the silicate additive. Further, the 300 g/ℓ goal was surpassed by such a large margin that the design point has been revised upward, to 350 g/ℓ.

SFUDS Testing

Zinc-air cell testing was also extended to include performance testing under the SFUDS cycle. The tests were conducted on the three-electrode cell, since its cathode's performance was close to the design goal for the system.

The test system comprised a set of power relays, resistors, a constant-current d.c. power supply, and a programmable controller. The cell voltage was recorded on a strip chart recorder. The programmable controller, *via* the power relays, connected the appropriate resistor (or the power supply for the regenerative braking periods) to achieve the specific power-time program shown in Figure 14.
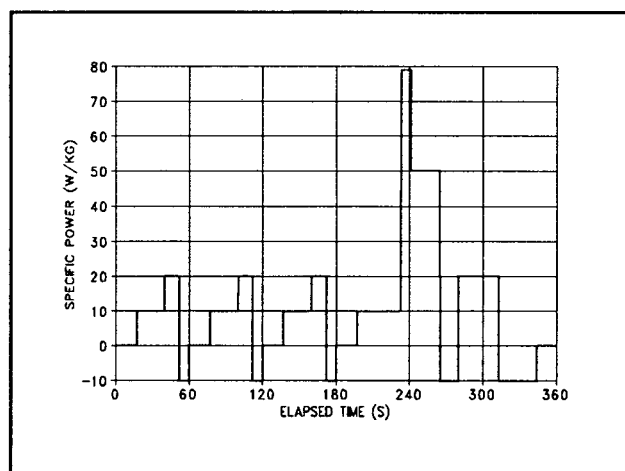
Figure 14: SFUDS Profile

The SFUDS cycle was run continuously on the cell from 100% state-of-charge (SOC) to 20% SOC. Figure 15 shows the resulting voltage-current density relationship at the two SOC's, and Figure 16 shows the power density-current density relationships. Figures 15 and 16 are based on the **minimum** voltage value for each step in the SFUDS cycle. The relationship between power density (mW/cm^2) and specific power (W/kg), based on the IDSEP Battery Design Specification, is as follows:

specific power = power density x 2.

Figure 16 shows that the 79 W/kg specific power (approximately 40 mW/cm^2 power density) is achieved at a current density of 35 mA/cm^2 at 100% SOC and at 38 mA/cm^2 at 20% SOC. Figure 15 shows that the voltages at these current densities are 1.17 V and 1.02 V, respectively, which are at least 80% of the nominal voltage of 1.2 V. Cell performance is therefore considered adequate for the SFUDS duty cycle.
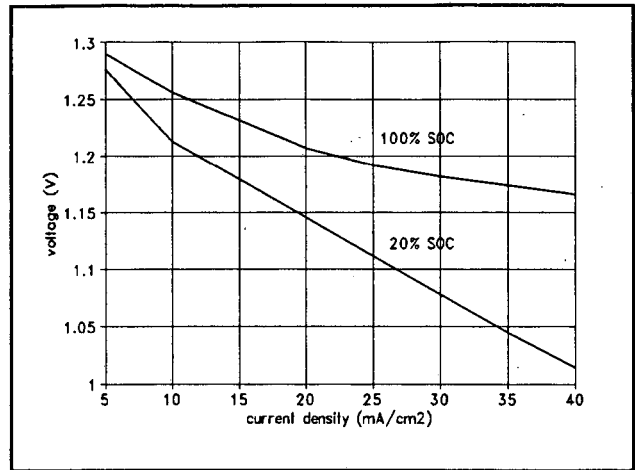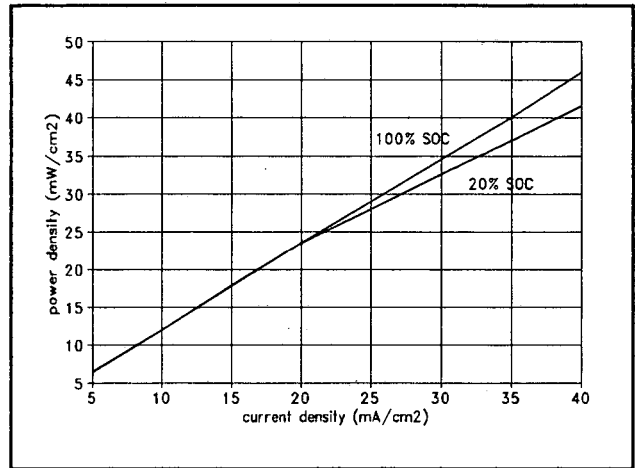

Figure 15: SFUDS Voltage-Current Curve

Figure 16: SFUDS Power-Current Curve

CONCLUSION

The metal foam zinc electrode has proven capable of extended (>700) cycle life absent densification. Moreover, because of electrolyte flow it avoids dryout failure in the open-system zinc-air battery, which would otherwise limit cycle life to less than 25 cycles. It requires a corrosion-resistant preplate of dense zinc, zinc-lead, or tin-lead to protect the copper substrate and to minimize hydrogen gassing. CELGARD 3401 is the best separator evaluated for this battery. Testing of zinc-air cells with three electrodes (an oxygen anode and cathode) showed that this approach, while feasible, is bulky and complex. Very encouraging results were obtained with rechargeable, or bifunctional, oxygen electrodes which employ graphitized catalyst supports and porphyrin and spinel electrocatalysts. Zinc-air cell testing showed satisfactory performance under the SFUDS duty cycle, and an electrolyte capacity of well over 350 g/ℓ of zinc solubility, as compared with a program target of 300 g/ℓ.

POSTSCRIPT

At the conclusion of the development program with Lawrence Berkeley Laboratory, MATSI began exploratory work to incorporate advances in the insoluble zinc electrode (Reference 4) into the metal foam design. The electrode was converted to an insoluble form by reducing the electrolyte volume by 40% and its concentration from 45% to 15%, along with the addition of supporting electrolytes such as potassium fluoride and potassium carbonate. The primary incentive for this was to increase specific energy; the specific energy for the soluble zinc electrode battery is projected to be 100 Wh/kg, while that for the insoluble zinc electrode battery is projected to be over 180 Wh/kg.

Recent (mid-1991) testing at LBL has shown that the insoluble zinc electrode, with low KOH concentrations and with supporting electrolyte additions, results in minimal shape change well beyond 500 cycles in nickel-zinc cells. Moreover, the foam substrate/electrolyte flow configuration of the present zinc-air battery permits periodic maintenance cycles, in which the zinc electrodes may be fully solubilized and stripped from the substrates, then recharged, thereby returning the zinc electrodes to their beginning-of-life condition.

Preliminary cycle testing of the insoluble form of the foam substrate electrode has been very successful. The zinc deposit is formed on the substrate by electrodeposition from a "soluble electrolyte" (concentrated KOH and zincate). We then switch to an "insoluble electrolyte" (3 M KOH saturated with zincate) and begin cycling, with electrolyte flow through the electrode to maintain moisture in the cell and to sweep out gas bubbles (entrained air and hydrogen generated at the zinc electrode). Periodically the "soluble electrolyte" is used to strip and re-deposit the zinc electrode. In practice this may be desirable every 100-200 cycles, depending on the rate of densification of the electrode.

Should this approach continue to prove practicable, it will make the zinc-air battery, by far, the highest of all aqueous rechargeable batteries in specific energy, and competitive with the specific energy claims for the lithium-polymer and lithium-iron disulfide systems. Beyond that, it demonstrates the value of the technology base research conducted at Lawrence Berkeley Laboratory, which has invented or developed the three key technologies making this approach possible, *i.e.* **the metal foam zinc electrode design, graphitized catalyst supports for rechargeable oxygen electrodes, and improvements to enhance the cycle life of the insoluble zinc electrode.**

REFERENCES

1. Putt, R.A., Zinc-Air Battery Development for Electric Vehicles: Final Report; LBL-29078, 1990.

2. Foller, P.C., _J. Appl. Electrochem._, Vol 16, pp 527-543, 1986.

3. Marshall, A. _et al_, _J. Elect. Chem._, Vol 59, p 33, 1975.

4. McLarnon, F., Lawrence Berkeley Laboratory, private communication, 1991.

APPENDIX A: ZINC-ZINC HALF CELL #1 TEST LOG

Test Period: 02/01/90 - 06/30/91

Initial Test Setup (continuation of Phase I testing):

● Working and Counter Electrodes (WE & CE): 3% dense Foametal® (Hogan Industries), preplated with dense zinc; 13 cm^2 area

● Separator: 2 layers of 3401 (Celgard)

● Electrolyte: 45% KOH with 50 g/ℓ zinc as zinc oxide

● Current Density: 5 mA/cm^2 charge and discharge

● Charge/Discharge Time: 8 h / 8 h

Date	MC#*	Comments/Observations
02/01/90	516	Start of Testing
02/07/90	525	Coated contact screws of WE with mercury to evaluate effect on system. Deposit became hard and dense.
02/09/90	528	Replaced separator with 2 layers of 3501 (Celgard), presuming that poor deposit morphology was due, in part, to the separator; it wasn't.
06/06/90	704	Morphology problems continued. Ascribed the problem to the presence of mercury. Replaced WE, at 704 cycles, with 6% dense Foametal, preplated with dense zinc. Replaced separator with 1 layer of 3401 to evaluate performance of 1 layer only.
06/22/90	728	Hard short developed. Replaced separator with 3 layers of 3401.
06/27/90	734	Voltage excursions at start of charge and discharge prompted the addition of PHDC80 (RAI) interlayers, between 3401 layers, to eliminate voids there.
07/19/90	769	Changed to a 6 h / 6 h charge/discharge cycle at 6 mA/cm^2 to reflect the IDSEP design duty cycle.

* Master Cycle Number; a sequential number beginning at the start of the original test program.

08/29/90	827	Replaced zinc-plated steel contact screws with solder-coated brass to eliminate gassing there.
09/04/90	838	Overtightened contact screw, which penetrated the CE, causing mechanical failure after 838 cycles. Replaced CE with 10 pore Retec (Eltech), preplated with dense zinc.
10/17/90	923	Observed that one layer of 3401 had ripped, and that one PHDC80 interlayer was laced with zinc. Replaced these with one layer each of 3401 and PHDC80.
11/13/90	976	Added lead oxide to reservoir to observe its effects on the electrodes. No observable changes occurred as a result.
11/15/90	979	Observed zinc deposit laced on interlayers. Machined the cell frames to compress the 3401 layers, thus allowing removal of the interlayers.
01/11/91	1090	Observed shorting during recharge opposite the oxygen evolving anode. Zinc deposit was dense, bright, nodular, and hard. Found that the KOH concentration was severely depleted by carbonation (electrolyte reservoir is not air-tight). Replaced electrolyte with fresh. Replaced separators, having 167 cycles, with 3 layers 3401.
06/30/91	1432	End of program. Cell continued to cycle, with 728, 592, and 342 cycles on the WE, CE and separator, respectively.

APPENDIX B: ZINC-ZINC HALF CELL #2 TEST LOG

Test Period: 02/01/90 - 06/30/91

Initial Test Setup (continuation of Phase I testing):

- Working and Counter Electrodes (WE and CE): 3% dense Foametal (Hogan Industries), preplated with dense zinc; 13 cm^2 area

- Separator: 1 layer of 3401, 2 layers of cellophane, 1 layer of 3401

- Electrolyte: 45% KOH with 50 g/ℓ zinc as zinc oxide

- Current Density: 5 mA/cm^2 charge and discharge

- Charge/Discharge Time: 8 h / 8 h

Date	MC#	Comments/Observations
02/01/90	516	Start of program.
04/03/90	609	Observed that only 1 layer of cellophane remained; the other had dissolved.
06/18/90	722	CE was overdischarged, zinc plating was gone, copper substrate was badly oxidized. Replaced CE, having 212 cycles, with 6% dense Foametal, preplated with dense zinc.
07/06/90	747	Conducted pulse plating trial on WE, using a 10% duty cycle, 15 Hz signal. This caused massive dendrite penetration of separator. Replaced separator, having 388 cycles, with 2 layers of 3401.
07/12/90	757	Observed voltage excursions at start of charge and discharge. Replaced separator, having 23 cycles, with 2 layers of 3401 bonded with polyvinyl alcohol. Did not eliminate the voltage excursions. Replaced separator with 2 layers of 5401 (Celgard).
07/16/90	763	Observed very high cell polarization. Observed that both electrodes were overdischarged. Stripped and replated both with dense zinc, replaced separator, having 23 cycles, with 3 layers of 5401.
08/10/90	798	Added 2 layers of PHDC80 (RAI) as interlayers to eliminate the voltage excursions. It didn't.

08/15/90	806	Replaced separator, having 20 cycles, with 2 layers of 3401 with one interlayer of PHDC80.
08/31/90	830	Both electrodes were overdischarged. WE had screw hole through it because of an overtightened contact screw. Replaced WE, having 472 cycles, with 10 pore Retec (Eltech), preplated with dense zinc. Observed gassing at zinc-plated steel contact screws, which was the cause of the overdischarge problem. Replaced contact screws with solder-coated brass screws. Replaced interlayer with one layer of 2515 (Pellon).
10/18/90	926	Replaced electrolyte with 45% KOH with 50 g/ℓ zinc as zinc oxide, plus 12 g/ℓ of Carbopol (B.F. Goodrich), a polymeric gelling agent, to evaluate its effect on the system.
11/06/90	964	Machined cell frames down to compress separator layers, removed interlayer.
11/08/90	967	Replaced electrolyte because of foaming of the Carbopol-containing electrolyte.
01/12/91	1092	Electrolyte was depleted of KOH because of carbonation (reservoir was not airtight). Replaced with fresh electrolyte.
02/15/91	1160	Indications of shorting. Machined cell frames down further to improve compression of separator layers, replaced separator after 354 cycles with 3 layers of 3401.
06/17/91	1406	Pump was inadvertently off during recharge, causing dendrite shorting. Replaced separator after 246 cycles with 3 layers of 3401.
06/30/91	1432	End of program. Cell continued to cycle, with 710, 602, and 26 cycles on the WE, CE, and separator, respectively.

LAWRENCE BERKELEY LABORATORY
UNIVERSITY OF CALIFORNIA
INFORMATION RESOURCES DEPARTMENT
BERKELEY, CALIFORNIA 94720